J. Phys.: Condens. Matter **22** (2010) 145701 (11pp) doi:10.1088/0953-8984/22/14/145701

Transport, magnetic, and ^{57}Fe and ^{155}Gd Mössbauer spectroscopic properties of GdFeAsO and the slightly overdoped superconductor $Gd_{0.84}Th_{0.16}FeAsO$

Pu Wang[1], Zbigniew M Stadnik[1], Cao Wang[2], Guang-Han Cao[2] and Zhu-An Xu[2]

[1] Department of Physics, University of Ottawa, Ottawa, ON, K1N 6N5, Canada
[2] Department of Physics, Zhejiang University, Hangzhou 310027, People's Republic of China

E-mail: stadnik@uottawa.ca

Received 23 December 2009, in final form 23 February 2010
Published 19 March 2010
Online at stacks.iop.org/JPhysCM/22/145701

Abstract

The results of x-ray diffraction, electrical resistivity, magnetic susceptibility, and ^{57}Fe and ^{155}Gd Mössbauer spectroscopy studies of polycrystalline samples of nonsuperconducting GdFeAsO and superconducting $Gd_{0.84}Th_{0.16}FeAsO$ are reported. The superconductor $Gd_{0.84}Th_{0.16}FeAsO$ has the onset transition temperature of 54.4(1) K. We find that Fe and Gd magnetic moments in GdFeAsO order antiferromagnetically at 132.7(1) K and 4.1(1) K, respectively. In $Gd_{0.84}Th_{0.16}FeAsO$, Fe atoms carry no magnetic moment down to 1.9 K whereas Gd magnetic moments order below 2.9(1) K. This is taken as evidence for the coexistence of Gd magnetic order and superconductivity. The Debye temperatures of GdFeAsO and $Gd_{0.84}Th_{0.16}FeAsO$ are, respectively, 409(4) and 389(3) K.

(Some figures in this article are in colour only in the electronic version)

1. Introduction

The dramatic discovery of superconductivity in Fe-based oxypnictides [1] $LaFeAsO_{1-x}F_x$ with a critical temperature T_c of 26 K has led to finding other high-temperature superconductors, such as $LnFeAsO_{1-x}F_x$ (Ln = rare earth) and $LnFeAsO_{1-\delta}$, with T_c as high as 55 K [2–5]. It was found that electron doping could also be realized by partial substitution of Ln by Th; this led to the discovery of the superconductors [6–9] $Ln_{1-x}Th_xFeAsO$ with T_c up to 56 K.

The parent nonsuperconducting compounds LnFeAsO are metallic antiferromagnets. Electron or hole doping of the parent compounds leads to the suppression of the static long-range antiferromagnetic order and the emergence of superconductivity [10, 11]. This is indicative of the interplay between magnetism and superconductivity in these compounds. The coexistence of Fe magnetism and superconductivity in the $LaFeAsO_{1-x}F_x$ superconductors has been claimed by Takeshita *et al* [12], but this has been disputed by Luetkens *et al* [13]. The coexistence of Fe magnetism and superconductivity has been reported for the $Ba_{1-x}K_xFe_2As_2$ [14–18] and $Ba(Fe_{1-x}Co_x)_2As_2$ [19] superconductors. The coexistence of superconductivity and the long-range antiferromagnetic order of Sm and Eu magnetic moments has been found in the $SmFeAsO_{1-x}F_x$ [20–23], $EuFe_2(As_{0.7}P_{0.3})_2$ [24] and $Eu_{0.5}K_{0.5}FeFe_2AsFe_2$ [25] superconductors, respectively.

Here we report the results of structural, electrical transport, and magnetic investigations of the parent compound GdFeAsO and its superconducting counterpart $Gd_{0.84}Th_{0.16}FeAsO$. The extreme absorption cross section of natural gadolinium precludes using neutron diffraction to study the magnetic order in Gd-containing compounds. The use of ^{57}Fe and ^{155}Gd Mössbauer spectroscopy (MS) allows us to explore the magnetic moments of Fe and Gd atoms in both compounds studied. We find the coexistence of magnetic ordering of the Gd magnetic moments with superconductivity below 2.9 K.

2. Experimental methods

Polycrystalline samples of nominal compositions GdFeAsO and $Gd_{0.75}Th_{0.25}FeAsO$ were synthesized as described earlier [6].

X-ray diffraction measurements were performed at 298 K in the Bragg–Brentano geometry on the PANanalytical X'Pert scanning diffractometer using Cu Kα radiation in the 2θ range 5°–100° in steps of 0.02°, with a graphite diffracted beam monochromator.

The electrical resistivity was measured with a standard four-probe method. The dc magnetic susceptibility was measured with a Quantum Design magnetic property measurement system (MPMS-5).

The ^{57}Fe and ^{155}Gd Mössbauer measurements were conducted using standard Mössbauer spectrometers operating in sine mode, with sources ^{57}Co(Rh) and ^{155}Eu($SmPd_3$), respectively. The ^{57}Co(Rh) source was at room temperature, whereas the ^{155}Eu($SmPd_3$) source was kept at the same temperature as that of the absorber. The ^{57}Fe and ^{155}Gd Mössbauer spectrometers were calibrated, respectively, with a 6.35 μm-thick α-Fe foil [26] and with a Michelson interferometer [27], and the spectra were folded. The full linewidth Γ at half maximum of the inner pair of the Zeeman pattern of the 6.35 μm-thick α-Fe foil measured with both Mössbauer spectrometers was 0.225(2) mm s^{-1}, and this value can be regarded as the resolution of the spectrometers used. The Mössbauer absorbers were made of pulverized material pressed into pellets (for ^{57}Fe Mössbauer absorbers, the pulverized material was mixed with boron nitride) which were then put into Al disk containers of thickness of 0.008 mm to ensure a uniform temperature over the whole sample. The surface densities of the ^{57}Fe Mössbauer absorbers of GdFeAsO and $Gd_{0.84}Th_{0.16}FeAsO$ were 12.5 and 13.3 mg cm^{-2}, whereas those of the ^{155}Gd Mössbauer absorbers were 250.6 and 265.0 mg cm^{-2}. The 14.4 and 86.5 keV γ-rays were detected, respectively, with a proportional counter and with a 2.5 cm NaI(Tl) scintillation detector covered with a 0.6 mm Pb plate to cut off the 105.3 keV γ-rays emitted from the ^{155}Eu($SmPd_3$) source.

The ^{57}Fe Mössbauer absorbers used here are thin [28]. Therefore, the ^{57}Fe Mössbauer spectra were analyzed in the thin-absorber approximation [28]. As the electric quadrupole interaction is significantly smaller than the dipole magnetic interaction in the studied compounds, the ^{57}Fe Zeeman spectra at temperatures much below the Néel temperature, T_N, were analyzed using the first-order perturbation treatment [28]. The ^{57}Fe Zeeman spectra at temperatures close to T_N are dynamic relaxation spectra (*vide infra*). They were therefore fitted with the formalism of Blume and Tjon [29].

The ^{155}Gd Mössbauer spectra were analyzed by means of a least-squares fitting procedure which entailed calculations of the positions and relative intensities of the absorption lines by numerical diagonalization of the full hyperfine interaction Hamiltonian. In the principal axis system of the electric field gradient (EFG) tensor, the Hamiltonian can be written as [28]

$$\hat{H} = g\mu_N H_{hf}[\hat{I}_z\cos\theta + \tfrac{1}{2}(\hat{I}_+ e^{-i\phi} + \hat{I}_- e^{i\phi})\sin\theta] + \frac{eQV_{zz}}{4I(2I-1)}\left[3\hat{I}_z^2 - I(I+1) + \frac{\eta}{2}(\hat{I}_+^2 + \hat{I}_-^2)\right], \quad (1)$$

where g is a nuclear g-factor of a nuclear state, μ_N is the nuclear Bohr magneton, H_{hf} is the hyperfine magnetic field at a nuclear site, Q is the quadrupole moment of a nuclear state, I is the nuclear spin, V_{zz} is the z component of the EFG tensor, η is the asymmetry parameter defined as $\eta = |(V_{xx} - V_{yy})/V_{zz}|$ (if the principal axes are chosen such that $|V_{xx}| < |V_{yy}| < |V_{zz}|$, then $0 \leqslant \eta \leqslant 1$), θ is the angle between the direction of H_{hf} and the V_{zz}-axis, ϕ is the angle between the V_{xx}-axis and the projection of H_{hf} onto the xy plane, and the $\hat{I}_z$, $\hat{I}_+$, and $\hat{I}_-$ operators have their usual meaning. During the fitting procedure, the g factor and the quadrupole moment ratios for ^{155}Gd ($I_g = 3/2$, $I_{ex} = 5/2$) were constrained to, respectively, $g_{ex}/g_g = 1.235$ and $Q_{ex}/Q_g = 0.087$ [30]. The interference factor ξ for the E1 transition of 86.5 keV in ^{155}Gd was fixed to the value of 0.0520, which was derived from the fit of the ^{155}Gd Mössbauer spectrum of $GdFe_2$ at 4.2 K [31].

The resonance line shape of the ^{155}Gd Mössbauer spectra was described by a transmission integral formula [32]. In addition to the hyperfine parameters, only the absorber Debye–Waller factor f_a and the absorber linewidth Γ_a were fitted as independent parameters. The source linewidth $\Gamma_s = 0.334$ mm s^{-1} and the background-corrected Debye–Waller factor of the source f_s^* [32], which were derived from the fit of the ^{155}Gd Mössbauer spectrum of $GdFe_2$ at 4.2 K [31], were used. The ^{155}Eu($SmPd_3$) source at 1.5 K emits a broadened emission line; from the fit of the ^{155}Gd Mössbauer spectrum of $GdFe_2$ at 1.5 K we found that $\Gamma_s = 0.708$ mm s^{-1} [31].

3. Experimental results and discussion

3.1. Structural characterization

The nonsuperconducting parent compound GdFeAsO crystallizes in the ZrCuSiAs-type crystal structure [33] with the tetragonal space group $P4/nmm$ (No. 129) [11]. There are 2 f.u. of GdFeAsO per unit cell. The room-temperature x-ray powder diffraction pattern of GdFeAsO is shown in figure 1. Table 1 lists the structural parameters of GdFeAsO obtained from the Rietveld refinement [34] of the spectrum in figure 1. The GdFeAsO specimen contains a second phase of As_2O_3 (space group $Fd\bar{3}m$) in the amount of 2.9(4) wt%, as determined from the Rietveld refinement. There is also a trace amount (estimated to be less than 1 wt%) of an unidentified impurity phase in the GdFeAsO specimen (figure 1). The resulting fit of the spectrum in figure 1 is reasonably good, as judged by the values of χ^2 and R factors (table 1). The lattice constants obtained from the Rietveld refinement, $a = 3.9170(3)$ Å and $c = 8.4526(4)$ Å, compare well with the values reported earlier [4, 6, 33]. Similarly to what has been observed for other parent compounds LnFeAsO [11], GdFeAsO is expected to experience a structural phase transition at ~135 K [6], changing the symmetry from tetragonal (space group $P4/nmm$) to orthorhombic (space group $Cmma$).

The superconducting compound of nominal composition $Gd_{0.75}Th_{0.25}FeAsO$ also crystallizes in the ZrCuSiAs-type crystal structure. The room-temperature x-ray powder diffraction pattern of $Gd_{0.75}Th_{0.25}FeAsO$ is shown in figure 2.

Table 1. Refined structural parameters of $Gd_{1-x}Th_xFeAsO$ with $x = 0$ and 0.25 at 298 K. Space group $P4/nmm$. For $x = 0$, $a = 3.9170(3)$ Å, $c = 8.4526(4)$ Å; for $x = 0.25$, $a = 3.9156(4)$ Å, $c = 8.4603(5)$ Å.

Atom	Site	Occup. ($x = 0$)	x	y	z ($x = 0$)	B (Å^2) ($x = 0$)	Occup. ($x = 0.25$)	z ($x = 0.25$)	B (Å^2) ($x = 0.25$)
Gd	2*c*	1.000	$\frac{1}{4}$	$\frac{1}{4}$	0.136(1)	0.10(1)	0.842(10)	0.138(2)	0.11(4)
Th	2*c*		$\frac{1}{4}$	$\frac{1}{4}$			0.158(9)	0.138(2)	0.11(4)
Fe	2*b*	1.000	$\frac{3}{4}$	$\frac{1}{4}$	$\frac{1}{2}$	0.39(2)	1.000		0.12(3)
As	2*c*	1.000	$\frac{1}{4}$	$\frac{1}{4}$	0.662(2)	0.36(2)	1.000	0.663(3)	0.09(3)
O	2*a*	1.000	$\frac{3}{4}$	$\frac{1}{4}$	0	1.0(1)	1.000		0.89(9)

For $x = 0$, $R_p = 4.84\%$, $R_{wp} = 4.10\%$, $\chi^2 = 1.36\%$
For $x = 0.25$, $R_p = 5.16\%$, $R_{wp} = 4.66\%$, $\chi^2 = 1.55\%$

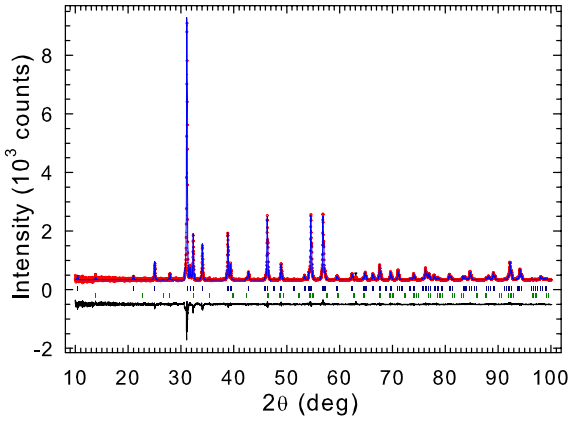

Figure 1. The x-ray diffraction spectrum of the nonsuperconducting parent compound GdFeAsO at 298 K. The experimental data are denoted by open circles, while the line through the circles represents the results of the Rietveld refinement. The upper set of vertical bars represents the Bragg peak positions corresponding to the GdFeAsO phase, while the lower set represents the positions of the impurity phase As_2O_3 (space group $Fd\bar{3}m$). The lower solid line represents the difference curve between experimental and calculated spectra. The symbol ▼ indicates the peak position corresponding to an unidentified impurity phase.

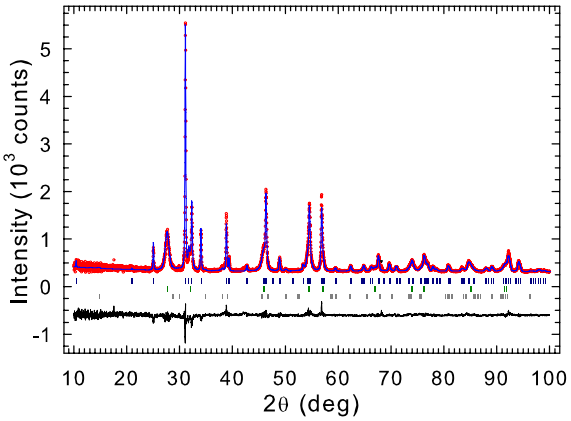

Figure 2. The x-ray diffraction spectrum of the superconducting compound $Gd_{0.84}Th_{0.16}FeAsO$ at 298 K. The experimental data are denoted by open circles, while the line through the circles represents the results of the Rietveld refinement. The upper set of vertical bars represents the Bragg peak positions corresponding to the principal $Gd_{0.84}Th_{0.16}FeAsO$ phase, while the lower two sets refer to the positions of the impurity phases of ThO_2 (space group $Fm\bar{3}m$) and Fe_2As (space group $P4/nmm$). The symbol ▼ indicates the peak position corresponding to an unidentified impurity phase.

The Rietveld refinement of the x-ray powder diffraction data was performed (figure 2), yielding the structural parameters listed in table 1. The specimen studied contains second phases of ThO_2 (space group $Fm\bar{3}m$) in the amount of 15.9(8) wt% and of Fe_2As (space group $P4/nmm$) in the amount of 5.6(4) wt%, as determined from the Rietveld refinement. In addition, there is a trace (estimated to be less than 3 wt%) of a third unidentified impurity phase in the studied specimen (figure 2). Rietveld analysis of the x-ray powder diffraction pattern of $Gd_{0.75}Th_{0.25}FeAsO$ (figure 2, table 1), with freely refined occupancies of Gd [0.842(10)] and Th [0.158(9)], yields a formula $Gd_{0.84}Th_{0.16}FeAsO$ for the compound of the nominal composition $Gd_{0.75}Th_{0.25}FeAsO$.

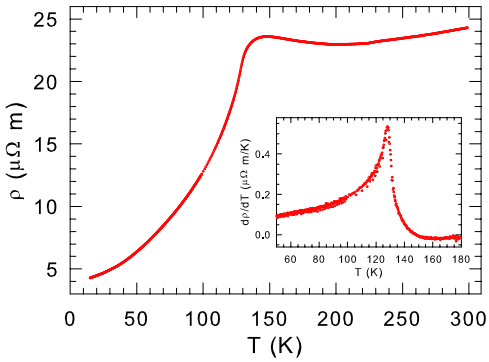

Figure 3. The temperature dependence of the electrical resistivity of GdFeAsO. The inset shows the temperature derivative of the measured electrical resistivity.

3.2. Electrical resistivity

Figure 3 shows the temperature dependence of the electrical resistivity ρ of GdFeAsO. At room temperature ρ has a value of 24.3 $\mu\Omega$ m, which decreases slightly upon cooling to ∼200 K. This value of ρ is typical for a low carrier-concentration metal or heavily doped semiconductor. Upon further cooling, ρ increases slightly reaching a broad maximum at the temperature $T_s = 148.2(2)$ K and drops rapidly below this temperature. A similar broad maximum in ρ was observed for LaFeAsO [35–37], PrFeAsO [38], and SmFeAsO [2] and the temperature T_s was associated with

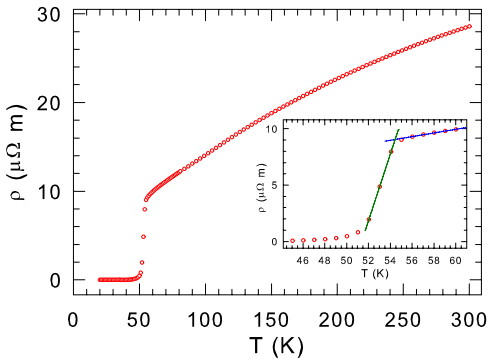

Figure 4. The temperature dependence of the electrical resistivity of $Gd_{0.84}Th_{0.16}FeAsO$. The inset shows the temperature dependence of the electrical resistivity near T_c. The intersection of the two lines defines T_c^{onset}, as explained in the text.

the structural phase transition from tetragonal to orthorhombic symmetry [2, 35–38]. We thus suggest that in GdFeAsO a tetragonal-to-orthorhombic structural phase transition occurs at 148.2(2) K.

The temperature dependence of $d\rho/dT$ (the inset of figure 3) exhibits a sharp maximum at the temperature $T^* = 128.2(2)$ K. The temperature T^* was shown to be close to the magnetic transition temperature T_N in LaFeAsO [35, 37]. The temperature T^* for GdFeAsO is indeed close to the T_N determined precisely with a local probe method (*vide infra*).

The temperature dependence of ρ for $Gd_{0.84}Th_{0.16}FeAsO$ is shown in figure 4. The onset T_c, T_c^{onset}, is determined from the intersection of the linear extrapolation of the most rapidly changing part of $\rho(T)$ and that of the normal-state $\rho(T)$, as shown in the inset of figure 4. The midpoint T_c, $T_c^{midpoint}$, is defined as the temperature at which the resistivity is 50% of its value at T_c^{onset}. The values of T_c^{onset} and $T_c^{midpoint}$ for $Gd_{0.84}Th_{0.16}FeAsO$ are 54.4(1) and 52.9(1) K, respectively (figure 4).

3.3. Magnetic susceptibility

The temperature dependence of the magnetic susceptibility χ of GeFeAsO measured in an applied magnetic field of 1 kOe is shown in figure 5(a). The sample was field-cooled to 2.0 K and the measurement was performed while warming the sample up to 300 K. The $\chi(T)$ curve exhibits a definite peak at 4.1(1) K, indicating antiferromagnetic ordering of Gd magnetic moments. The $\chi(T)$ data above 70 K could be fitted to a modified Curie–Weiss law

$$\chi = \chi_0 + \frac{C}{T - \Theta_p}, \qquad (2)$$

where χ_0 is the temperature-independent magnetic susceptibility, C is the Curie constant, and Θ_p is the paramagnetic Curie temperature. The Curie constant can be expressed as $C = \frac{N\mu_{eff}^2}{3k_B}$, where N is the number of Gd ions/f.u., μ_{eff} is the effective magnetic moment, and k_B is the Boltzmann constant. Figure 5(b) shows the inverse magnetic susceptibility corrected for the contribution χ_0 as $(\chi - \chi_0)^{-1}$

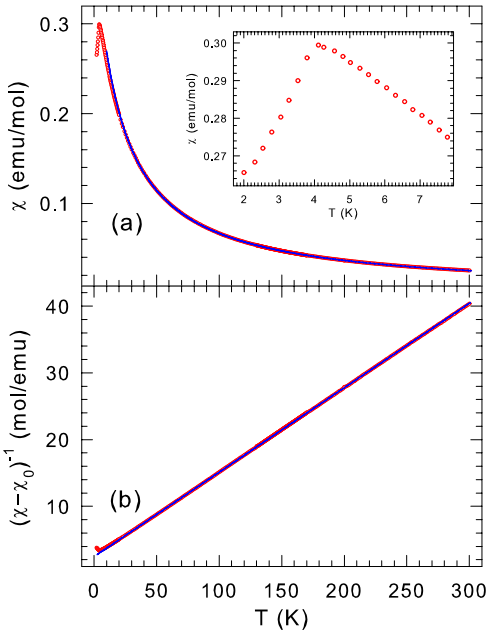

Figure 5. (a) The temperature dependence of the magnetic susceptibility of GdFeAsO measured in an external magnetic field of 1 kOe. The solid line is the fit to equation (2) in the temperature range 30–300 K, as explained in the text. The inset shows the magnetic susceptibility data in the low-temperature range. (b) The inverse magnetic susceptibility corrected for the contribution χ_0, $(\chi - \chi_0)^{-1}$ versus temperature T. The solid line is the fit to equation (2).

versus temperature; the validity of the modified Curie–Weiss law is evident. The values of χ_0, C, and Θ_p obtained from the fit are, respectively, $5.88(20) \times 10^{-4}$ emu mol^{-1}, 7.90(1) emu K mol^{-1}, and $-19.3(1)$ K. A relatively large value of χ_0 results most probably from the unidentified Fe-containing magnetic impurity phase present in the our sample. The value of C corresponds to $\mu_{eff} = 7.95(1)\ \mu_B$ per Gd atom.

For a free Gd^{3+} ion (electronic configuration $^8S_{7/2}$), the theoretical value of $\mu_{eff}^{th} = g\mu_B\sqrt{J(J+1)}$ is 7.94 μ_B [39]. The fact that the experimental value $\mu_{eff} = 7.95(1)\ \mu_B$ is very close to the theoretical value of 7.94 μ_B confirms that the magnetic moment is localized on the Gd^{3+} ions. The negative value of Θ_p indicates the predominantly antiferromagnetic interaction between the Gd^{3+} magnetic moments.

Figure 6 shows the temperature dependence of the zero-field-cooled (ZFC) and field-cooled (FC) magnetic susceptibility of $Gd_{0.84}Th_{0.16}FeAsO$ measured in an applied magnetic field of 10 Oe. A sharp drop of the ZFC and FC χ curve below 52.3(1) K confirms the superconducting nature of the compound. Clearly, the presence of ferromagnetic impurities in the sample contributes to a temperature-independent background signal which shifts the ZFC and FC $\chi(T)$ data upwards. One observes a sharp increase of the ZFC χ below 2.9(1) K (inset of figure 6). This is indicative of the magnetic ordering of the Gd^{3+} magnetic moments below 2.9(1) K in the $Gd_{0.84}Th_{0.16}FeAsO$ superconductor. The presence of such an ordering is directly confirmed by the ^{155}Gd MS results described below.

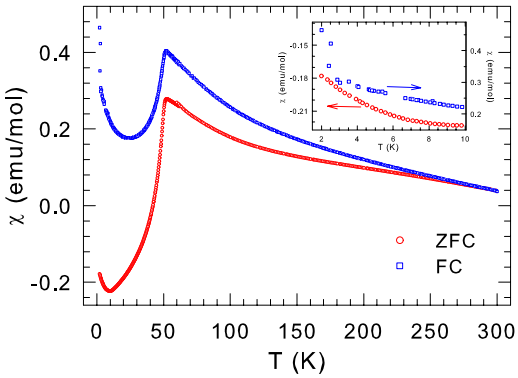

Figure 6. The temperature dependence of the ZFC and FC magnetic susceptibility of $Gd_{0.84}Th_{0.16}FeAsO$ measured in an external magnetic field of 10 Oe. The inset shows a magnification of the low-temperature region.

3.4. Mössbauer spectroscopy

The ^{57}Fe Mössbauer spectra of the GdFeAsO sample recorded at temperatures at which no magnetic dipole hyperfine interaction [28] is present in the GdFeAsO compound are shown in figure 7. The spectra can be fitted with a single Lorentzian line corresponding to the GdFeAsO phase and a weak Zeeman pattern resulting from an unknown Fe-containing impurity phase present in the specimen (figure 1). The value of Γ of the singlet changes from 0.260(2) mm s^{-1} at 298.4 K to 0.273(8) mm s^{-1} at 133.9 K. This proves that the quadrupole interaction is negligible in this temperature range.

Figure 8 shows the ^{57}Fe Mössbauer spectra of the GdFeAsO specimen measured at temperatures at which the magnetic dipole hyperfine interaction [28] is present in the GdFeAsO compound. Between 1.9 and 119.1 K, the ^{57}Fe Mössbauer spectra of GdFeAsO are in the form of a simple magnetic sextet resulting from the static Zeeman pattern corresponding to the GdFeAsO phase and a weak Zeeman pattern resulting from an unknown Fe-containing impurity phase present in the specimen. At 1.9 K, the center shift δ (relative to α-Fe at 298 K), the quadrupole shift ϵ [28], and the hyperfine magnetic field $H_{\rm hf}$ are 0.542(4) mm s^{-1}, $-0.035(1)$ mm s^{-1}, and 49.93(10) kOe, respectively. The values of these three hyperfine parameters indicate that Fe atoms are likely in a low-spin Fe(II) electronic configuration [28]. The symmetry of the ^{57}Fe Mössbauer spectra of GdFeAsO (figures 1 and 2) indicates that Fe is also divalent in the Fe-containing impurity.

The ^{57}Fe Mössbauer spectra of GdFeAsO between 124.4 and 131.4 K are more complex (figure 8) and cannot be fitted with a simple static Zeeman pattern and a weak Zeeman pattern corresponding to the impurity phase. Similar complex ^{57}Fe Mössbauer spectra at temperatures close to $T_{\rm N}$ have been observed for the LaFeAsO parent compound [35, 37, 40]. These complex spectra could, in principle, be modeled with a distribution of $H_{\rm hf}$ resulting from a possible incommensurate/commensurate spin-density wave developed below $T_{\rm N}$ [41]. This, however, cannot be right: the very fact that the spectra below 119.1 K can be well described with a simple magnetic sextet indicates the absence of spin-density wave behavior. Using an Overhauser line profile given by Daniels *et al* [42], an ^{57}Fe incommensurate spin-density wave Mössbauer spectrum was generated with $H_{\rm hf} = 40.0$ kOe, $\delta = 0.520$ mm s^{-1}, $\epsilon = -0.035$ mm s^{-1}, and $\Gamma = 0.273$ mm s^{-1} (figure 9). Although the shape of this generated spectrum is similar to that of the experimental spectra above 119.1 K (figure 8), its central part is significantly more intense than that of the experimental spectra. We therefore believe that the ^{57}Fe Mössbauer spectra between 124.4 and 131.4 K are spin relaxation spectra resulting from the fluctuations of $H_{\rm hf}$ [43]. Excellent fits of these Mössbauer spectra were obtained (figure 8) using the line shape function for the pattern corresponding to the GdFeAsO phase given by Blume and Tjon [29] and a weak Zeeman pattern corresponding to the impurity phase.

The temperature dependence of $H_{\rm hf}$ derived from the fits of the Mössbauer spectra in figure 8 is presented in figure 10. The temperature at which $H_{\rm hf}$ vanishes, which was obtained from the spline extrapolation of the $H_{\rm hf}(T)$ data in figure 10, is $T_{\rm N} = 132.7(1)$ K. It compares well with the $T_{\rm N}$ values determined from neutron diffraction studies for LaFeAsO (137 K) [41, 44], CeFeAsO (140 K) [11, 45], PrFeAsO (127 K) [46], NdFeAsO (141(6) K) [47], and from muon spin rotation studies for SmFeAsO (138 K) [20].

The value of $H_{\rm hf}$ at 0 K, which was derived from the spline extrapolation of the $H_{\rm hf}(T)$ data in figure 10, is $H_{\rm hf}(0) = 49.94(10)$ kOe. The measured $H_{\rm hf}$ is, to a first approximation, proportional to the on-site magnetic moment of iron atoms $\mu_{\rm Fe}$ via the relation $H_{\rm hf} = a\mu_{\rm Fe}$, where the proportionality constant a is in the range 125–150 kOe/$\mu_{\rm B}$ and its value is compound specific [28, 48]. In converting $H_{\rm hf}$ to $\mu_{\rm Fe}$, we used $a = 144$ kOe/$\mu_{\rm B}$, which results from $H_{\rm hf}(4.2\ {\rm K}) = 51.9(1)$ kOe measured for LaFeAsO [37] and $\mu_{\rm Fe}(8\ {\rm K}) = 0.36(5)\ \mu_{\rm B}$ determined from the neutron diffraction study of LaFeAsO [41]. The hyperfine magnetic field $H_{\rm hf}(0) = 49.94(5)$ kOe corresponds then to $\mu_{\rm Fe}(0) = 0.346(1)\ \mu_{\rm B}$. Similarly small values of $\mu_{\rm Fe}$ were determined from neutron diffraction studies of LaFeAsO (0.36(5) $\mu_{\rm B}$) [41], CeFeAsO (0.83(2) $\mu_{\rm B}$) [45], PrFeAsO (0.48(9) $\mu_{\rm B}$ [46], 0.53(20) $\mu_{\rm B}$ [38]), and NdFeAsO (0.25(7) $\mu_{\rm B}$) [47].

The temperature dependence of $\delta(T)$, determined from the fits of the Mössbauer spectra in figures 7 and 8, is shown in figure 11. $\delta(T)$ is given by

$$\delta(T) = \delta_0 + \delta_{\rm SOD}(T), \tag{3}$$

where δ_0 is the intrinsic isomer shift and $\delta_{\rm SOD}(T)$ is the second-order Doppler (SOD) shift which depends on lattice vibrations of the Fe atoms [28]. In terms of the Debye approximation of the lattice vibrations, $\delta_{\rm SOD}(T)$ is expressed [28] by the Debye temperature, $\Theta_{\rm D}$, as

$$\delta_{\rm SOD}(T) = -\frac{9}{2}\frac{k_{\rm B}T}{Mc}\left(\frac{T}{\Theta_{\rm D}}\right)^3 \int_0^{\Theta_{\rm D}/T} \frac{x^3\,{\rm d}x}{{\rm e}^x - 1}, \tag{4}$$

where M is the mass of the Mössbauer nucleus and c is the speed of light. By fitting the experimental data (figure 11)

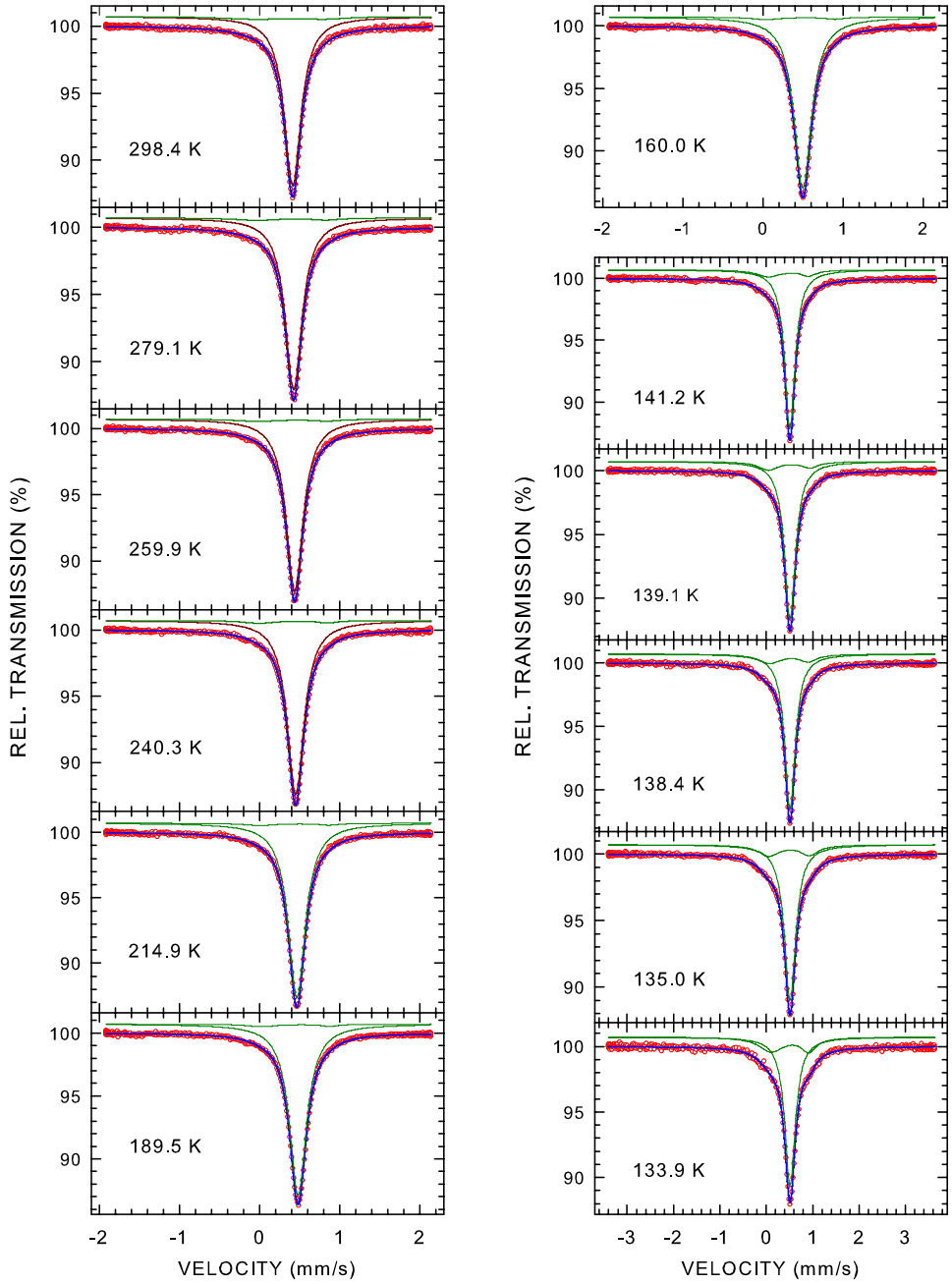

Figure 7. The ^{57}Fe Mössbauer spectra of GdFeAsO obtained at the indicated temperatures fitted (solid lines) with a singlet pattern corresponding to the GdFeAsO phase and a weak Zeeman pattern corresponding to the unidentified impurity phase. The zero-velocity origin is relative to α-Fe at room temperature.

to equation (3), the quantities δ_0 and Θ_D were found to be, respectively, 0.540(2) mm s^{-1} and 409(4) K.

Figure 12 displays the ^{155}Gd Mössbauer spectra of GdFeAsO measured at temperatures at which the magnetic dipole hyperfine interaction [28] is absent. The Gd atoms are located at the 4g site (space group *Cmma*) with the point symmetry *mm*2, which ensures a non-zero EFG at this site, and hence a non-zero electric quadrupole hyperfine interaction. The Mössbauer spectra in figure 12 indeed exhibit the presence of a substantial electric quadrupole hyperfine interaction. For ^{155}Gd nuclei, the quadrupole moment of the excited nuclear state $Q_{ex} = 0.12b$ [30] is significantly smaller than that of the ground nuclear state $Q_g = 1.30b$ [49]. As a result, the quadrupole splitting of the excited nuclear state, which is sensitive to the sign of V_{zz} and the magnitude of η, is smaller than the natural linewidth $\Gamma_{nat} = 0.250$ mm s^{-1} and thus is not resolved. Consequently, only the absolute value of the effective quadrupole splitting parameter $\Delta_g^{eff} = eQ_g|V_{zz}|\sqrt{1+\eta^2/3}$ can be derived from a Mössbauer spectrum, which has the appearance of a doublet [50]. The following values of the hyperfine parameters were inferred from the fit of the 4.3 K Mössbauer spectrum: $\delta = 0.489(4)$ mm s^{-1} (relative to the ^{155}Eu(SmPd$_3$) source), $\Delta_g^{eff} = 4.121(15)$ mm s^{-1}, $f_a = 14.2(4)\%$, and $\Gamma_a = 0.294(16)$ mm s^{-1}. The value

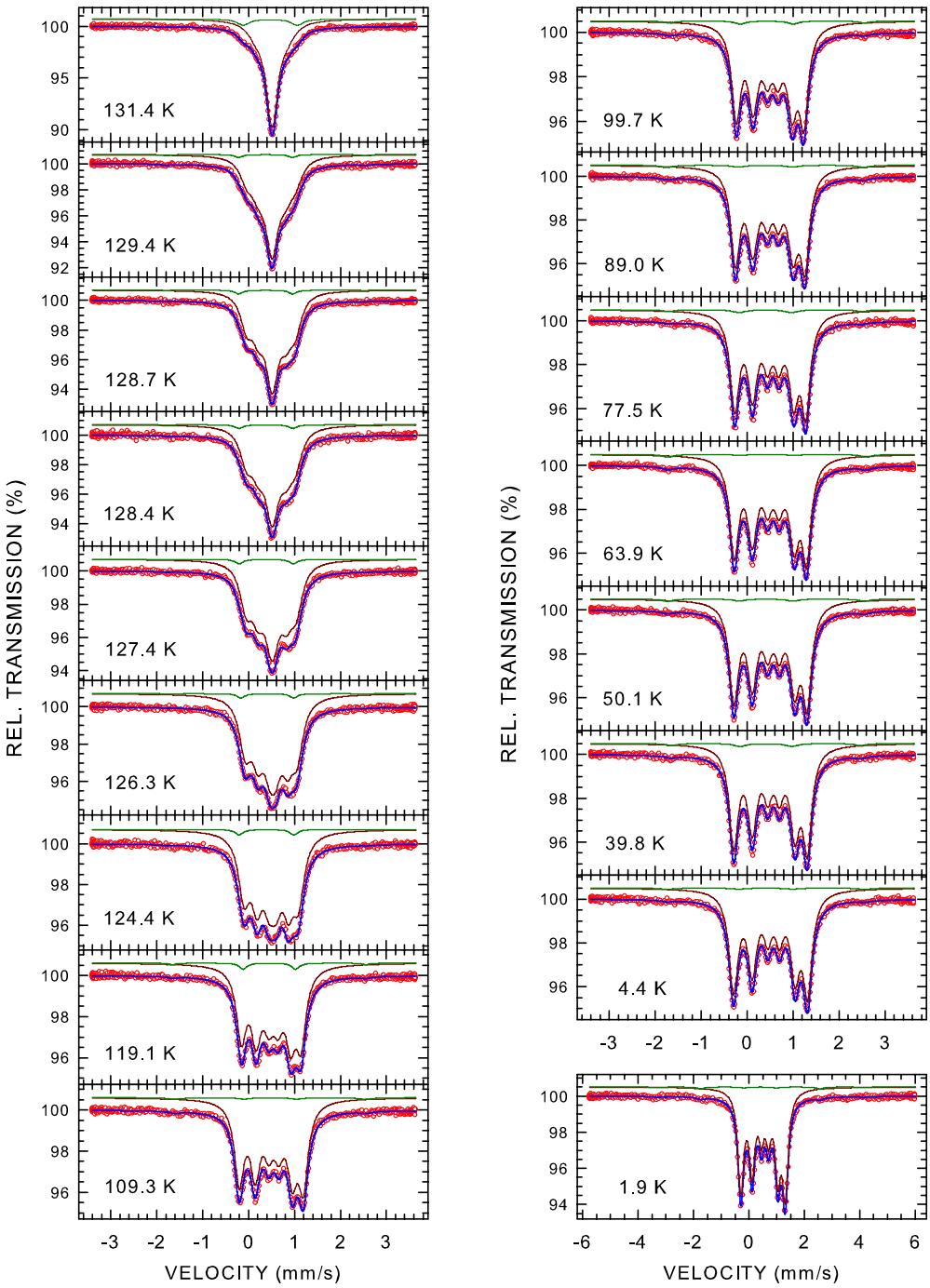

Figure 8. The ^{57}Fe Mössbauer spectra of GdFeAsO obtained at the indicated temperatures. The full lines are the fits with a Zeeman pattern corresponding to the GdFeAsO phase and a weak Zeeman pattern corresponding to the unidentified impurity phase. The zero-velocity origin is relative to α-Fe at room temperature.

of δ confirms the trivalent state of Gd in the GdFeAsO compound [50]. The absence of the magnetic dipole hyperfine interaction in the Mössbauer spectra in figure 12 proves that the Gd magnetic moments are not ordered down to 4.3 K.

The ^{155}Gd Mössbauer spectrum of GdFeAsO measured at 1.5 K clearly shows (figure 13) the presence of a combined magnetic dipole and electric quadrupole hyperfine interactions. The presence of the magnetic dipole hyperfine interaction in the Mössbauer spectrum in figure 13 proves that at 1.5 K the Gd magnetic moments are ordered. The parameters derived from the fit of the Mössbauer spectrum (figure 13) are: $\delta = 0.468(11)$ mm s^{-1}, $H_{\rm hf} = 277.5(7.7)$ kOe, the quadrupole splitting constant $eQ_{\rm g}V_{zz} = -3.401(151)$ mm s^{-1} ($V_{zz} = -7.55(34) \times 10^{21}$ V cm^{-2}), $\eta = 0.99(19)$, $\theta = 46.1(2.5)°$, $f_{\rm a} = 15.8(9)\%$, and $\Gamma_{\rm a} = 0.255(26)$ mm s^{-1}. A substantial value of $H_{\rm hf}$ indicates that the Gd atoms have a considerable magnetic moment.

Figure 14 shows the ^{57}Fe Mössbauer spectra of $Gd_{0.84}Th_{0.16}FeAsO$ measured at different temperatures in the range 1.9–299.1 K. These spectra could be modeled well as

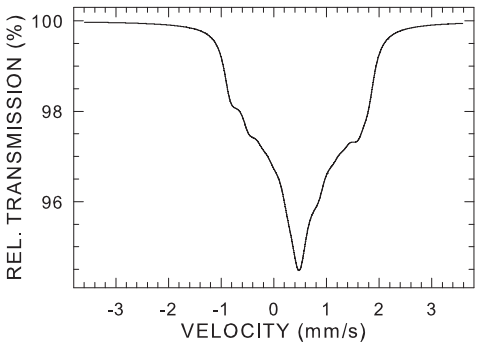

Figure 9. The incommensurate spin-density wave ^{57}Fe Mössbauer spectrum generated using the Overhauser line profile [42] with $H_{\rm hf} = 40.0$ kOe, $\delta = 0.520$ mm s^{-1}, $\epsilon = -0.035$ mm s^{-1}, and $\Gamma = 0.273$ mm s^{-1}.

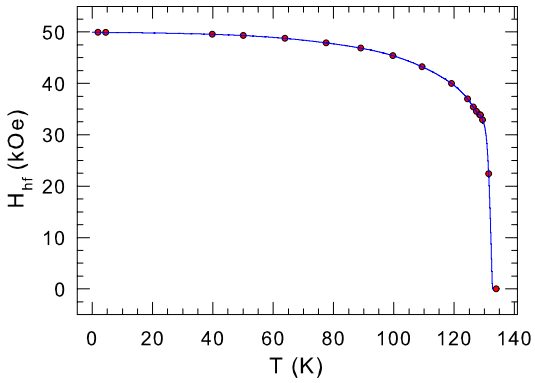

Figure 10. The temperature dependence of the hyperfine magnetic field of GdFeAsO. The solid line is a guide for the eyes. The experimental point at 133.9 K corresponds to $H_{\rm hf} = 0$.

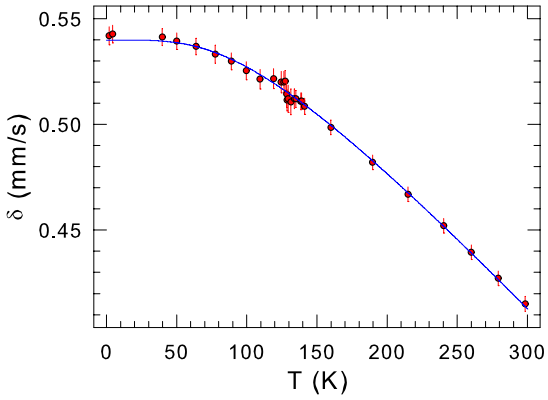

Figure 11. The temperature dependence of the center shift δ of GdFeAsO. The solid line is the fit to equation (2), as explained in the text.

a superposition of two Zeeman patterns originating from the Fe_2As impurity (the precise set of hyperfine parameters of the two inequivalent Fe sites in Fe_2As at different temperatures was taken from [51]), a Zeeman pattern associated with an unidentified Fe-containing impurity (figure 2), and a singlet corresponding to the $Gd_{0.84}Th_{0.16}FeAsO$ phase. The spectral areas corresponding to the Fe_2As and the unidentified Fe-

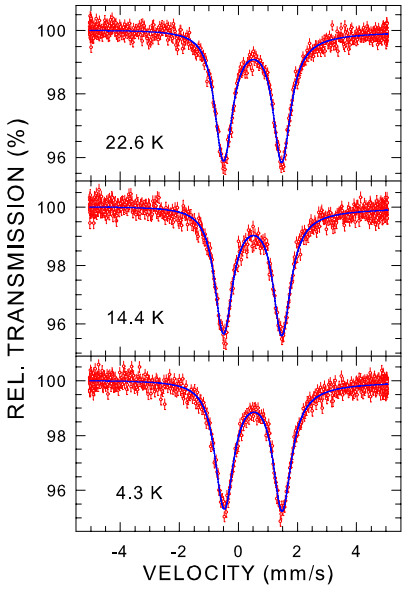

Figure 12. The ^{155}Gd Mössbauer spectra of GdFeAsO obtained at the indicated temperatures. The full lines are the fits, as described in the text. The zero-velocity origin is relative to the source.

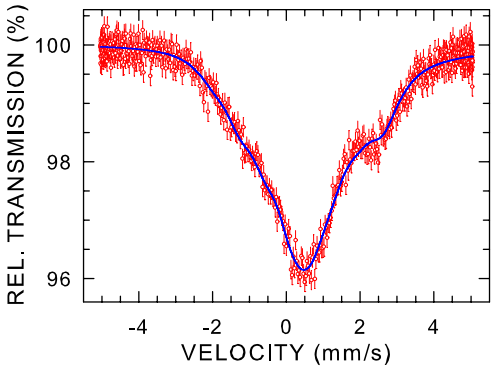

Figure 13. The ^{155}Gd Mössbauer spectrum of GdFeAsO at 1.5 K fitted (solid line) with a combined magnetic dipole and electric quadrupole hyperfine interactions. The zero-velocity origin is relative to the source.

containing impurity phases are, respectively, about 8 and 4%, in a reasonable agreement with the Rietveld results. The presence of a singlet down to 1.9 K proves that Fe atoms carry no magnetic moment, i.e., there is no magnetic order associated with the Fe atoms down to 1.9 K.

The temperature dependence of δ, derived from the fits of the Mössbauer spectra in figure 14, is shown in figure 15. The fit of the experimental data $\delta(T)$ (figure 15) to equation (3) yields $\delta_0 = 0.552(2)$ mm s^{-1} and $\Theta_{\rm D} = 389(3)$ K. The values of δ_0 and $\Theta_{\rm D}$ for $Gd_{0.84}Th_{0.16}FeAsO$ are very similar to those for GdFeAsO and close to the corresponding values for the $NdFeAsO_{0.82}F_{0.18}$ superconductor [52].

Figure 16 shows the ^{155}Gd Mössbauer spectra of $Gd_{0.84}Th_{0.16}FeAsO$ at 15.8 and 4.2 K. Clearly, no magnetic dipole hyperfine interaction is present at those temperatures. Thus, the Gd magnetic moment is zero down to 4.2 K. The fit of the 4.2 K Mössbauer spectrum yields $\delta = 0.482(4)$ mm s^{-1},

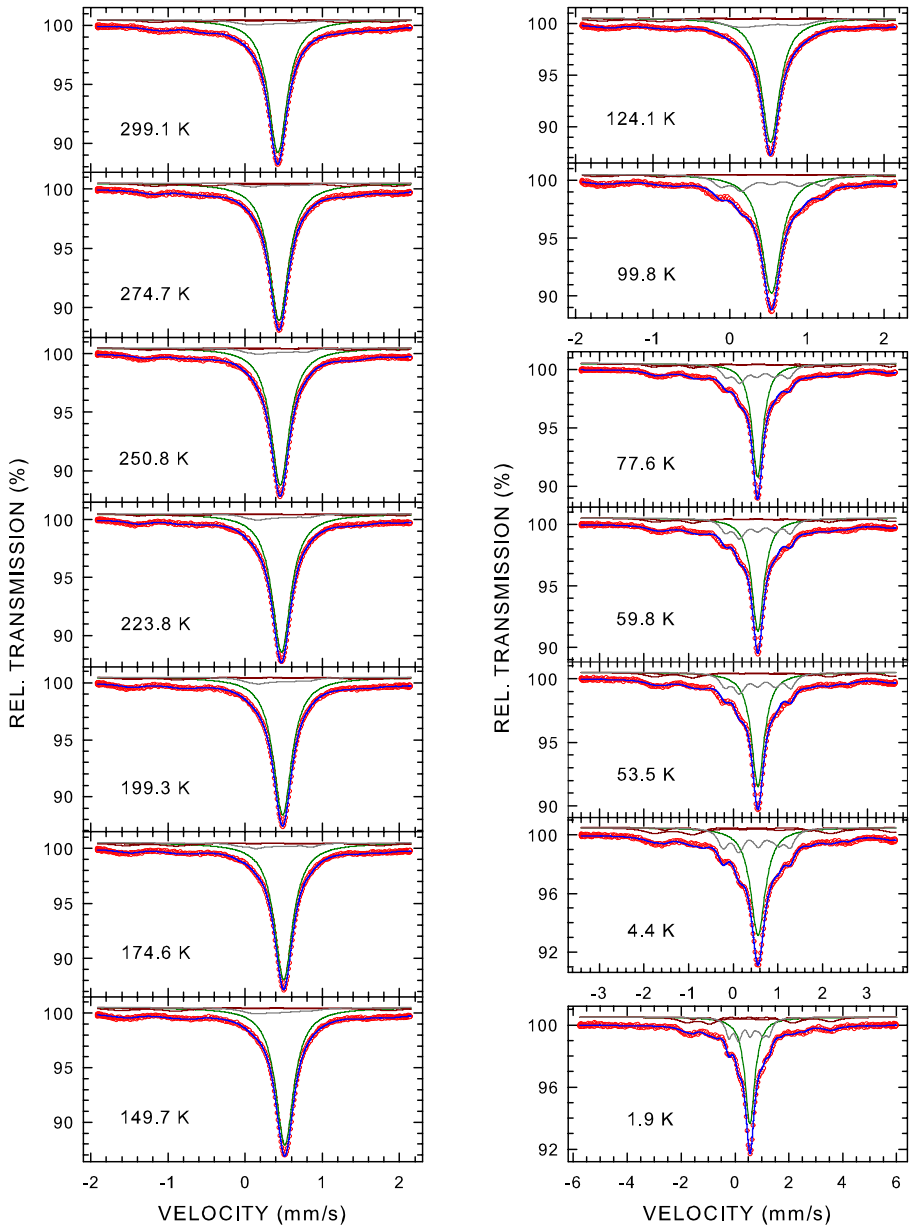

Figure 14. The ^{57}Fe Mössbauer spectra of $Gd_{0.84}Th_{0.16}FeAsO$ obtained at the indicated temperatures fitted (solid lines) with a singlet corresponding to the $Gd_{0.84}Th_{0.16}FeAsO$ phase, two Zeeman patterns associated with the Fe_2As impurity, and a Zeeman pattern corresponding to another unidentified impurity phase. The zero-velocity origin is relative to α-Fe at room temperature.

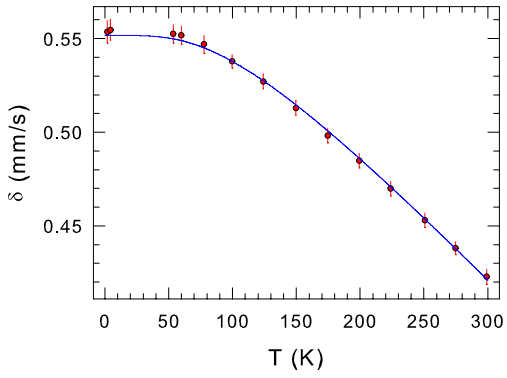

Figure 15. The temperature dependence of the center shift δ of $Gd_{0.84}Th_{0.16}FeAsO$. The solid line is the fit to equation (2), as explained in the text.

$\Delta_g^{eff} = 3.702(16)$ mm s^{-1}, $f_a = 14.2(2)\%$, and $\Gamma_a = 0.394(11)$ mm s^{-1}. The values of δ and f_a for $Gd_{0.84}Th_{0.16}FeAsO$ are quite similar to the corresponding values for GdFeAsO. The value of Δ_g^{eff} for $Gd_{0.84}Th_{0.16}FeAsO$ is about 10% smaller than that for GdFeAsO. The larger value of Γ_a for $Gd_{0.84}Th_{0.16}FeAsO$ than for GdFeAsO is expected: it results from the disorder caused by the substitution of the Gd by the Th atoms.

The ^{155}Gd Mössbauer spectrum of $Gd_{0.84}Th_{0.16}FeAsO$ measured at 1.5 K is shown in figure 17. The presence of the magnetic dipole hyperfine interaction in this spectrum is evident. The following values of the hyperfine parameters were inferred from the fit of this spectrum (the value of $\Gamma_a = 0.394$ mm s^{-1}, which was taken from the fit of the 4.2 K spectrum, was fixed in this fit): $\delta = 0.491(12)$ mm s^{-1},

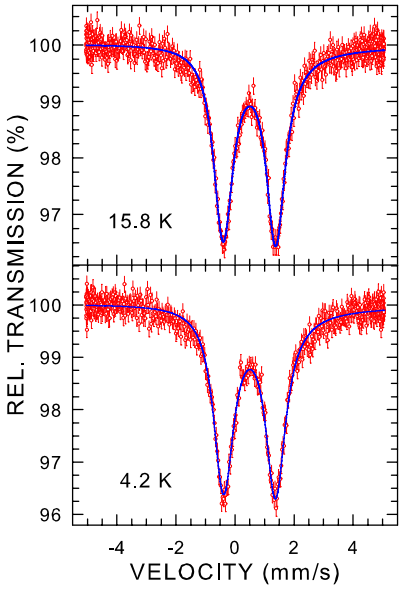

Figure 16. The ^{155}Gd Mössbauer spectra of $Gd_{0.84}Th_{0.16}FeAsO$ obtained at the indicated temperatures. The full lines are the fits, as described in the text. The zero-velocity origin is relative to the source.

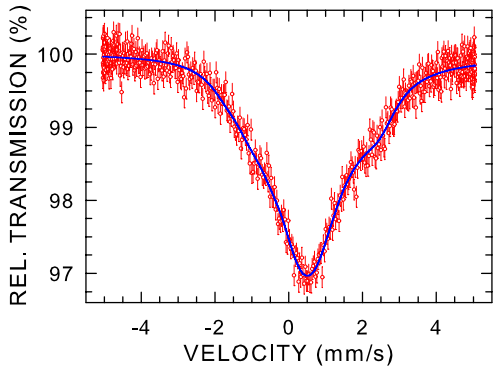

Figure 17. The ^{155}Gd Mössbauer spectrum of $Gd_{0.84}Th_{0.16}FeAsO$ at 1.5 K fitted (solid line) with a combined magnetic dipole and electric quadrupole hyperfine interactions. The zero-velocity origin is relative to the source.

$H_{hf} = 245.9(11.5)$ kOe, $eQ_gV_{zz} = -3.021(235)$ mm s^{-1} ($V_{zz} = -6.70(52) \times 10^{21}$ V cm^{-2}), $\eta = 0.99(33)$, $\theta = 51.0(3.9)°$, and $f_a = 15.3(9)\%$. A considerable value of H_{hf} indicates a substantial magnetic moment of the Gd atoms at 1.5 K. This demonstrates unequivocally the coexistence of superconductivity and magnetic order of the Gd atoms in the $Gd_{0.84}Th_{0.16}FeAsO$ superconductor.

4. Conclusions

We report the results of x-ray diffraction, electrical resistivity, magnetic susceptibility, and ^{57}Fe and ^{155}Gd Mössbauer spectroscopy measurements of the nonsuperconducting GdFeAsO and superconducting $Gd_{0.84}Th_{0.16}FeAsO$. It is shown that in GdFeAsO the Fe magnetic moments order antiferromagnetically at 132.7(1) K and the Gd magnetic moments order at 4.1(1) K. No evidence for the presence of spin-density waves is found in the ^{57}Fe Mössbauer spectra of GdFeAsO. In $Gd_{0.84}Th_{0.16}FeAsO$, the Fe atoms are shown to carry no magnetic moment down to 1.9 K and the Gd magnetic moments order below 2.9(1) K. This demonstrates the coexistence of superconductivity and the magnetic order of the Gd atoms in the $Gd_{0.84}Th_{0.16}FeAsO$ superconductor. The Debye temperatures of GdFeAsO and $Gd_{0.84}Th_{0.16}FeAsO$ are found to be 409(4) and 389(3) K, respectively.

Acknowledgments

This work was supported by the Natural Sciences and Engineering Research Council of Canada, the National Scientific Foundation of China, and the National Basic Research Program of China (Contract No. 2007CB925001). The authors wish to thank Dr J Żukrowski for informative discussions and helpful advice.

References

[1] Kamihara Y, Watanabe T, Hirano M and Hosono H 2008 *J. Am. Chem. Soc.* **130** 3296
[2] Ren Z A *et al* 2008 *Chin. Phys. Lett.* **25** 2215
Liu R H *et al* 2008 *Phys. Rev. Lett.* **101** 087001
[3] Ren Z A, Che G C, Dong X L, Yang J, Lu W, Li W, Shen X L and Li Z C 2008 *Europhys. Lett.* **83** 17002
Kito H, Eisaki H and Iyo A 2008 *J. Phys. Soc. Japan* **77** 063707
[4] Yang J *et al* 2008 *Supercond. Sci. Technol.* **21** 082001
[5] Miyazawa K, Kihou K, Shirage P M, Lee C H, Kito H, Eisaki H and Iyo A 2009 *J. Phys. Soc. Japan* **78** 034712
[6] Wang C *et al* 2008 *Europhys. Lett.* **83** 67006
[7] Li L J, Li Y K, Ren Z, Luo Y K, Lin X, He M, Tao Q, Zhu Z W, Cao G H and Xu Z A 2008 *Phys. Rev.* B **78** 132506
[8] Xu M, Chen F, He C, Ou H W, Zhao J F and Feng D L 2008 *Chem. Mater.* **20** 7201
[9] Prakash J, Singh S J, Patnaik S and Ganguli A K 2009 *J. Phys.: Condens. Matter* **21** 175705
[10] Ishida K, Nakai Y and Hosono H 2009 *J. Phys. Soc. Japan* **78** 062001 and references therein
[11] Lynn J W and Dai P 2009 *Physica* C **460** 469 and references therein
[12] Takeshita S, Kadono R, Hiraishi M, Miyazaki M, Koda A, Kamihara Y and Hosono H 2008 *J. Phys. Soc. Japan* **77** 103703
Takeshita S and Kadono R 2009 *New J. Phys.* **11** 035006
[13] Luetkens H *et al* 2009 *Nat. Mater.* **8** 305
[14] Aczel A A *et al* 2008 *Phys. Rev.* B **78** 214503
[15] Chen H *et al* 2009 *Europhys. Lett.* **85** 17006
[16] Park J T *et al* 2009 *Phys. Rev. Lett.* **102** 117006
[17] Goko T *et al* 2009 *Phys. Rev.* B **80** 024508
[18] Rotter M, Tegel M, Schellenberg I, Schappacher F M, Pöttgen R, Deisenhofer J, Günther A, Schrettle F, Loidl A and Johrendt D 2009 *New J. Phys.* **11** 025014
[19] Laplace Y, Bobroff J, Rullier-Albenque F, Colson D and Forget A 2009 *Phys. Rev.* B **80** 140501(R)
[20] Drew A J *et al* 2009 *Nat. Mater.* **8** 310
[21] Margadonna S, Takabayashi Y, McDonald M T, Brunelli M, Wu G, Liu R H, Chen X H and Prassides K 2009 *Phys. Rev.* B **79** 014503
[22] Sanna S, De Renzi R, Lamura G, Ferdeghini C, Palenzona A, Putti M, Tropeano M and Shiroka T 2009 *Phys. Rev.* B **80** 052503

[23] Ding L, He C, Dong J K, Wu T, Liu R H, Chen X H and Li S Y 2009 *Phys. Rev.* B **77** 180510(R)
[24] Ren Z, Tao Q, Jiang S, Feng C, Wang C, Dai J, Cao G and Xu Z 2009 *Phys. Rev. Lett.* **102** 137002
[25] Anupam, Paulose P L, Jeevan H S, Geibel C and Hossain Z 2009 *J. Phys.: Condens. Matter* **21** 265701
[26] Cali J P (ed) 1971 *Certificate of Calibration, Iron Foil Mössbauer Standard* (Washington, DC: US GPO) Natl. Bur. Stand. (U.S.) Circ. No. 1541
[27] Otterloo B F, Stadnik Z M and Swolfs A E M 1983 *Rev. Sci. Instrum.* **54** 1575
[28] Greenwood N N and Gibb T C 1971 *Mössbauer Spectroscopy* (London: Chapman and Hall)
Gütlich P, Link R and Trautwein A 1978 *Mössbauer Spectroscopy and Transition Metal Chemistry* (Berlin: Springer)
[29] Blume M and Tjon J A 1968 *Phys. Rev.* **165** 446
[30] Armon H, Bauminger E R and Ofer S 1973 *Phys. Lett.* B **43** 380
[31] Stadnik Z M and Żukrowski J 2005 unpublished
[32] Margulies S and Ehrman J R 1961 *Nucl. Instrum. Methods* **12** 131
Shenoy G K, Friedt J M, Maletta H and Ruby S L 1974 *Mössbauer Effect Methodology* vol 10, ed I J Gruverman, C W Seidel and D K Dieterly (New York: Plenum) p 277
[33] Johnson V and Jeitschko W 1974 *J. Solid State Chem.* **11** 161
Zimmer B I, Jeitschko W, Albering J H, Glaum R and Reehuis M 1995 *J. Alloys Compounds* **229** 238
Quebe P, Terbüchte L J and Jeitschko W 2000 *J. Alloys Compounds* **302** 70
[34] Young R A 1993 *The Rietveld Method* (Oxford: Oxford University Press)
[35] Klauss H-H *et al* 2008 *Phys. Rev. Lett.* **101** 077005
[36] Dong J *et al* 2008 *Europhys. Lett.* **83** 27006
[37] McGuire M A *et al* 2008 *Phys. Rev.* B **78** 094517
[38] Kimber S A J *et al* 2008 *Phys. Rev.* B **78** 140503(R)
[39] Ashcroft N W and Mermin N D 1976 *Solid State Physics* (Philadelphia, PA: Saunders)
[40] Kitao S, Kobayashi Y, Higashitaniguchi S, Saito M, Kamihara Y, Hirano M, Mitsui T, Hosono H and Seto M 2008 *J. Phys. Soc. Japan* **77** 103706
[41] de la Cruz C *et al* 2008 *Nature* **453** 899
[42] Daniels J M, Julian S R, Lam H-Y and Li P L 1985 *Can. J. Phys.* **63** 409
[43] Rancourt D G 1996 *Mössbauer Spectroscopy Applied to Magnetism and Materials Science* vol 2, ed G J Long and F Grandjean (New York: Plenum) p 105
[44] Huang Q, Zhao J, Lynn J W, Chen G F, Luo J L, Wang N L and Dai P 2008 *Phys. Rev.* B **78** 054529
[45] Zhao J *et al* 2008 *Nat. Mater.* **7** 953
[46] Zhao J *et al* 2008 *Phys. Rev.* B **78** 132504
[47] Chen Y, Lynn J W, Li J, Li G, Chen G F, Luo J L, Wang N L, Dai P, de la Cruz C and Mook H A 2008 *Phys. Rev.* B **78** 064515
[48] Panissod P, Durand J and Budnik J I 1982 *Nucl. Instrum. Methods* **199** 99
Panissod P 1985 *Hyperfine Interact.* **24–26** 607
Eriksson O and Svane A 1989 *J. Phys.: Condens. Matter* **1** 1589
[49] Tanaka Y, Laubacher D B, Steffen R M, Shera E B, Wohlfahrt H D and Hoehn M V 1982 *Phys. Lett.* B **108** 8
[50] Czjzek G 1993 *Mössbauer Spectroscopy Applied to Magnetism and Materials Science* vol 1, ed G J Long and F Grandjean (New York: Plenum) p 373
[51] Rancourt D G, Daniels J M and Lam H-Y 1985 *Can. J. Phys.* **63** 1540
[52] Pissas M, Sanakis Y, Psycharis V, Simopoulos A, Devlin E, Ren Z A, Shen X L, Che G C and Zhao Z X 2008 *Supercond. Sci. Technol.* **21** 115015